J Mol Model (2011) 17:1635–1641
DOI 10.1007/s00894-010-0867-5

ORIGINAL PAPER

Molecular dynamics studies of human receptor molecule in hemagglutinin of 1918 and 2009 H1N1 influenza viruses

Angelina Noviani Lee · Yossa Dwi Hartono · Tiedong Sun · Min Li Leow · Xue-wei Liu · Xuri Huang · Dawei Zhang

Received: 25 August 2010 / Accepted: 1 October 2010 / Published online: 27 October 2010

Abstract Molecular dynamics (MD) simulations were carried out to study the behavior of human receptor molecule in the hemagglutinin (HA) of 1918 and 2009 H1N1 influenza viruses respectively. The 2009 HA model was obtained by virtually mutating the 1918 HA crystal structure based on A/Mexico City/MCIG01/2009(H1N1) segment 4 sequence. We found that human receptor molecule has no binding preference between the 2009 HA and the 1918 HA. In addition, among the four sugar moieties in the human receptor molecule, sialic acid contributes the most to the electrostatic and non-polar interaction energy during binding. Furthermore, the hydrogen bonds between sialic acid and the surrounding residues in 1918 HA are preserved in 2009 HA. We also found that the mutated residues contribute to a more favorable binding of hemagglutinin to the human receptor molecule.

Keywords 2009 H1N1 hemagglutinin · Human receptor molecule · Sialic acid

Electronic supplementary material The online version of this article (doi:10.1007/s00894-010-0867-5) contains supplementary material, which is available to authorized users.

A. N. Lee · Y. D. Hartono · M. L. Leow · X.-w. Liu · D. Zhang (✉)
Division of Chemistry and Biological Chemistry,
School of Physical and Mathematical Sciences,
Nanyang Technological University,
Singapore 637371, Singapore
e-mail: zhangdw@ntu.edu.sg

T. Sun · X. Huang (✉)
State Key Laboratory of Theoretical and Computational Chemistry, Institute of Theoretical Chemistry, Jilin University,
Changchun 130023, People's Republic of China
e-mail: huangxr@jlu.edu.cn

Introduction

Influenza A viruses are classified based on the combination of their two viral surface antigens: hemagglutinin and neuraminidase, of which 16 (H1–H16 HA) and 9 (N1–N9 NA) are known to date, respectively. Hemagglutinin facilitates the attachment of virus to the cell surface and the entry of viral RNA into the host cell [1, 2], whereas neuraminidase aids the release of virus from the infected cells.[3, 4] The H1N1 influenza virus responsible for the recent 2009 pandemic is a novel virus of avian/human/swine 'quadruple reassortants' [5]. This virus has caused at least 18,366 deaths since it was first identified in April 2009 [6]. Currently, there are two recommended FDA-approved antiviral drugs (oseltamivir phosphate and zanamivir) against 2009 H1N1 virus and both drugs inhibit only the neuraminidase of the virus [7]. It should be noted that the inhibition of neuraminidase only stops the release of virus, but does not stop the viral entry. The treatment leaves the host cell practically infected due to the biological activity of hemagglutinin. Furthermore, there have been reported cases of oseltamivir-resistant H1N1 virus [6], prompting a need to study the hemagglutinin as a new target. Hence, this project is carried out to gain a better understanding on the binding of H1N1 hemagglutinin (H1 HA) to the human receptor molecule.

Studies done by Hancock et al. [8] and Itoh et al. [9] suggested that older adults who were exposed to '1918-like H1N1' virus have antibodies against the 2009 pandemic H1N1. This observation lead us to think that the hemagglutinin structure of 2009 H1N1 virus would be similar to that of 1918 H1N1. Hence, we mutated the 1918 H1 HA based on the A/Mexico City/MCIG01/2009(H1N1) segment 4 sequence to make the 2009 H1 HA model. In this project, we focus on the molecular dynamics of the human

receptor molecule in both 1918 and 2009 H1 HA. Using computational methods, the following comparisons are made for both hemagglutinins: 1) binding affinity to human receptor molecule and interaction energy contributions of individual sugar moieties, 2) hydrogen bond pattern for individual sugar moieties, and 3) interaction energy of individual residues in the hemagglutinin to the human receptor molecule.

When our study was near the end stage, Xu et al. [10] managed to obtain the crystal structure (PDB id 3LZG) of the hemagglutinin from A/California/04/2009 H1N1 virus. To evaluate the similarities between the crystal structure and our predicted structure for the 2009 H1 HA, the backbone atoms and the sequence for both hemagglutinin were aligned. We found that the HA1 domain, which contains the glycan binding site, for both structures differ by only three residues. The RMSD value between the two structures (1.39 Å for HA1) is also relatively small and within the range of experimental uncertainties. These data shows that the approximated 2009 H1 HA structure that we made for this study is quite accurate. Hence, we believe that the subsequent insightful studies that we have done herein are still relevant and valid.

Methods

Hemagglutinin system setups

The co-crystal structure of 1918 HA monomer and human receptor molecule was obtained from PDB (PDB id 2WRG) [11] while the structure of 2009 HA monomer was obtained by virtually mutating the 1918 HA crystal structure based on A/Mexico City/MCIG01/2009(H1N1) segment 4 sequence using Maestro 8.0 [12] followed by 5 ns MD simulation with a partial solvation approach to completely relax the mutated structure. Afterward, one can easily dock the human receptor molecule into 2009 HA monomer by simply superimposing it over the complex structure of 1918 HA and human receptor molecule.

Molecular dynamics (MD) simulations

All MD simulations were carried out using SANDER module of AMBER 9 program [13] with FF03 force field [14] for the proteins and GLYCAM06 force field [15] for the glycans. For both complex structures, the area around the HA head (HA1 domain) was subjected to partial explicit solvation with 35 Å of solvation radius from the center of the globular HA head. To prevent the inner water molecules from escaping into the surrounding, water molecules within the outer 5 Å radius were restrained. K^+ ions were added to maintain the electro-neutrality of the system. The direct-space, nonbonded cutoff was set to 12.0 Å. The simulation based on this cutoff was compared with the one with a larger cutoff radius (20.0 Å) to check the convergence of the free energy of binding values for 1918 HA. It turned out that the two simulation results with a cutoff of 12 Å and 20 Å respectively are similar in terms of RMSD fluctuation and SIE determined binding free energy (shown in S1 in the supporting information). Minimization was done in two steps: solvent minimization while the HA and the human receptor molecule were fixed, and then the whole system minimization. Both steps were done by steepest descent, followed by conjugate gradient minimization. The time step for equilibration was set to 2.0 fs and bonds involving hydrogen atom were constrained using SHAKE algorithm [16]. The equilibration was carried out using weak-coupling ensemble [17] and the time constant for heat bath coupling was set to 2.0 ps. During equilibration, only molecules within the 30 Å radius of the globular HA center were allowed to move while the coordinates of the rest were frozen. The system was heated up from 10.0 K to 300.0 K over 100 ps, and then a subsequent isobaric-isothermal production was done over 20 ns. Water molecules and K^+ ions were then stripped off from the trajectory and RMSD analysis were done to find the region with less fluctuations for free energy calculations. All simulation images were generated using VMD [18].

Free energy calculations

Free energy was calculated by averaging the solvated interaction energy (SIE) using Sietraj program [19, 20]. Sietraj is an alternative to the MM-PBSA calculation in AMBER 9 [13]. This method is related most closely to the linear interaction energy (LIE) approach first proposed by Åqvist et al. [21]. According to this method, the binding free energy is written as a linear combination of the electrostatic interaction energy between the protein and the ligand, E_{elec}, and the difference of the reaction field energies of the complex, the receptor and the isolated ligand, ΔG_{bind}^{reac}, and the van der Waals interaction energy, E_{vdW}, and the change in the molecular surface area upon binding, ΔMBA.

$$\begin{aligned}\Delta G_{bind} &= \alpha(E_{elec} + \Delta G_{bind}^{reac} + E_{vdW} + \gamma \Delta MSA) + C \\ &= 0.1048 \times [E_{elec} + \Delta G_{bind}^{reac} + E_{vdW} + 0.0129 \times \Delta MSA] - 2.89\end{aligned} \quad (1)$$

The coefficients of these energy terms are calibrated by fitting to the absolute binding free energies for a set of 99 protein–ligand complexes [20]. The first two terms represent the electrostatic contribution to the binding free energy, and the last two terms account for the non-polar contribu-

Fig. 1 Comparison of 1918 and 2009 H1N1 HA sequence. The mutations are framed in red

tion to the binding free energy. The energy terms included in the linear equation are obtained by averaging over a series of snapshots from MD trajectories with the program sietraj, and the weighting terms are fitted to experimental binding free energies. There is no explicit entropic term in the equation; the entropic contribution to the binding free energy is taken into account implicitly through the weighting coefficients and the constant. In our studies, the SIE were averaged over 1000 snapshots that were collected every 10 structures from the trajectory of the last 10 ns. We believe that this 10 ns productive run having stable fluctuation and recording the coordinates every 10 ps will be sufficiently far apart that the structures are uncorrelated. In order to test it, we carried out a trial SIE calculation by using 2000 snapshots from the trajectory of the last 15 ns. As we can see from S2 in the supporting information, the results from the two selections of the snapshots are quite similar. It is understandable because the RMSD fluctuations (shown in Fig. 2) for both the receptor and the ligand are stable after 5 ns simulation.

Hydrogen bond analysis

Hydrogen bond analysis was carried out using Ptraj program of AMBER 9 [13]. Intra-residue interactions were not included. A distance cut-off of 3.00 Å (donor-acceptor) and angle cut-off of 120.00 degree (donor-H-acceptor) were used as hydrogen bond criteria. Only hydrogen bonds that exist more than 5% of the investigated time period, i.e., more than 5% occupancy, are reported. The sugar images were drawn using ChemBioDraw Ultra 11 [22].

Results and discussion

We used the 1918 H1 HA structure obtained from the Protein Data Bank (PDB ID: 2WRG) as a template to create the 2009 H1 HA model for this project based on A/Mexico City/MCIG01/2009(H1N1) segment 4 sequence. The sequences for 1918 and predicted 2009 H1 HA were aligned and the comparison is shown in Fig. 1. We found that there is an

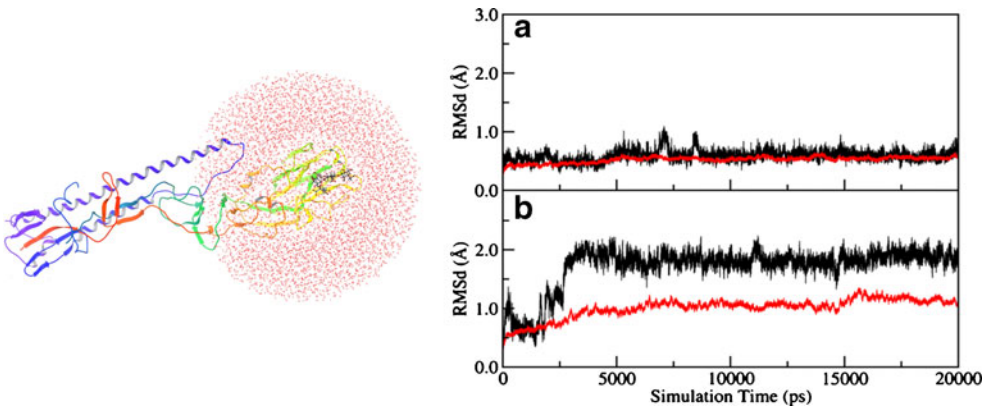

Fig. 2 Left: 1918 H1N1 HA under partial solvation. Right: root-mean-square deviations (Å) of human receptor and **a**) 1918 HA, **b**) 2009 HA. Red line: hemagglutinin, black line: human receptor

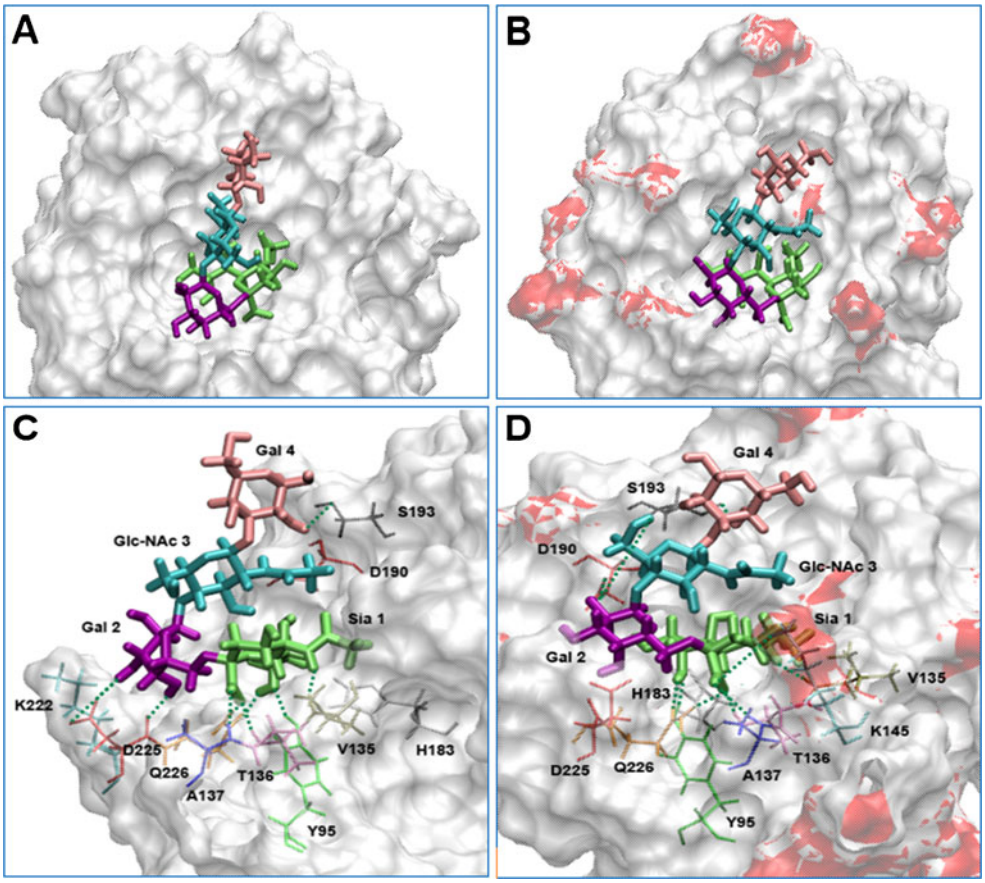

Fig. 3 Starting conformation for MD simulation: **a**) 1918 HA and **b**) 2009 HA. Last frame of 20 ns simulation: **c**) 1918 HA and **d**) 2009 HA. Mutated residues of the predicted 2009 HA are highlighted in red. The green dashed lines represent the hydrogen bonds

overall similarity of 86.0% between both sequences, which consists of 82.8% similarity in HA1 region and 92.5% similarity in HA2 region. This high percentage of similarity suggests that the degree of mutation is low considering the number of decades that has lapsed.

Both hemagglutinin – human receptor complexes were then subjected to partial explicit solvation (refer to Fig. 2 left panel) to reduce computational cost for MD simulation. Full explicit solvation would be too costly because a huge amount of water molecules and a lot of time are required to fully simulate the whole system. Twenty nanoseconds of MD simulation were then performed for both 1918 and 2009 system. The RMSD analysis performed after the simulation shows that both systems were well equilibrated after 5 ns with relatively small-ranged fluctuations (less than 0.5 Å) as depicted in Fig. 2 right panel. The 2009 RMSD plot shows a great jump in value compared to the 1918 plot, indicating a large deviation from the starting conformation. This deviation can be explained by the fact that we determine the complex structure of 2009 HA and human receptor molecule by structural alignment rather than molecule docking. As a result when the simulation was carried out, there were adjustments in the 2009 system to reach the lowest energy conformation. From the region with the least fluctuation in the RMSD plot, 1000 snapshots were collected from each system for further analyses.

The comparison of 1918 and 2009 binding site is illustrated in Fig. 3 a & b with the mutated residues highlighted in red. These mutations have caused conformational change of the bound human receptor molecule and

Table 1 Binding free energy components for the hemagglutinin – human receptor complex

Contribution	1918 complex		2009 complex	
	Mean[a]	σ[b]	Mean[a]	σ[b]
E_{vdW}	−33.39	3.32	−41.09	3.61
E_{elec}	−54.29	5.30	−79.27	8.60
ΔG_{RF}	52.20	4.03	80.09	6.42
ΔG_{npsol}	−6.58	0.33	−8.88	0.36
ΔG	−7.30	0.35	−8.04	0.44

All values are given in kcal mol^{-1} [a] Average over 1000 snapshots

[b] Standard error of mean values. The σ values for E_{vdW}, E_{elec}, ΔG_{RF}, *and* ΔG_{npsol} are the values before applying weighting terms

E_{vdW} : intermolecular van der Waals interaction energies in the bound state

E_{elec}: intermolecular coulombic interaction energies in the bound state

ΔG_{RF}: change in reaction field energy between the bound and free states

ΔG_{npsol}: the change in the non-electrostatic solvation energy between the bound and free states

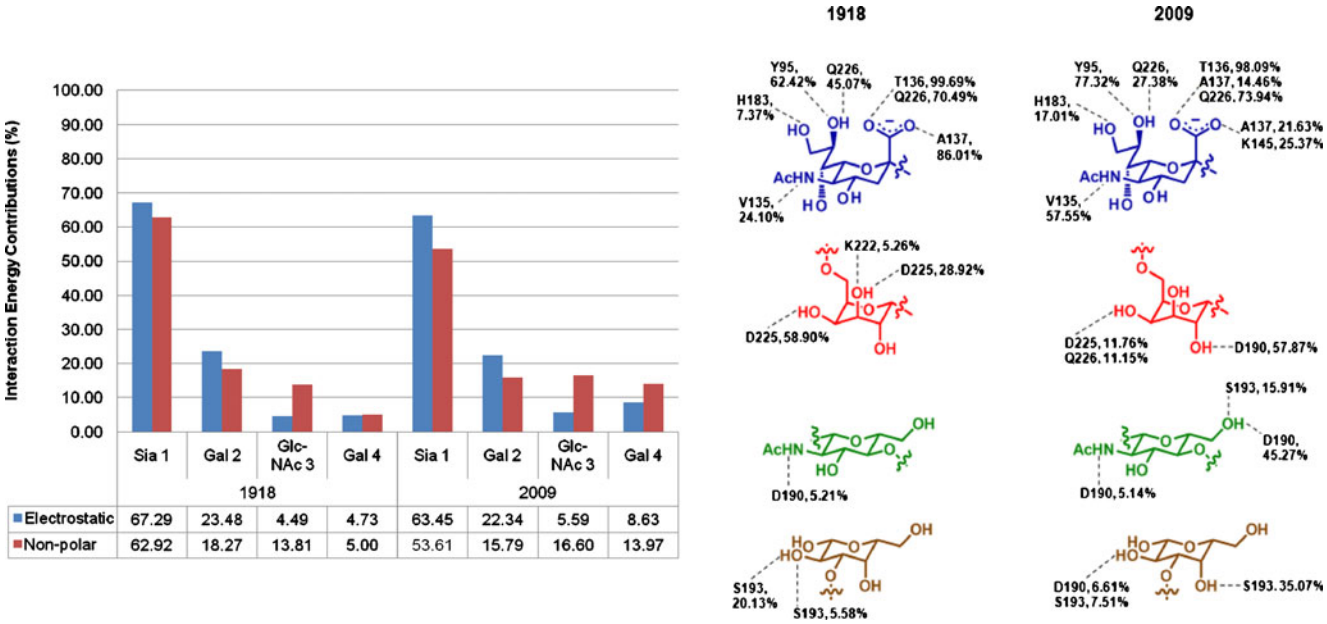

Fig. 4 Left: Comparison of interaction energy components of individual sugar moieties. Right: hydrogen bond pattern for individual sugar moiety. Top-bottom: Sia 1, Gal 2, Glc-NAc 3, Gal 4. The dashed line represents hydrogen bond between the protein and the individual sugar moiety. If there is more than one hydrogen bond formed from a donor/acceptor atom to the same residue, only the largest occupancy value is shown

eventually, the change in interactions of individual sugar moieties with the surrounding amino acid residues. Fig. 3 c & d shows some of the changes in binding interaction, especially the loss of hydrogen bonds to D225 residue in 2009 HA. The snapshots in Fig. 3, however, do not really give much detail as they are only static figures taken from the last frame of the MD simulation. The hemagglutinin–human receptor system, on the contrary, is a dynamic system whereby some hydrogen bonds break and re-formed while others stay intact along the simulation period. Thus, binding free energy calculation and hydrogen bond analysis were performed to obtain more detailed information on binding interaction.

The binding free energies calculated for both systems are listed in Table 1. The values are estimated using solvated interaction energy (SIE) approach [19, 20] as in Eq. 1. In our case, the binding free energy of the 2009 complex (-8.04 kcal mol^{-1}) is relatively similar to that of the 1918 complex (-7.30 kcal mol^{-1}), implying that both 1918 and 2009 H1 HA have similar binding affinity to human receptor molecule. The percentage breakdown of electrostatic E_{elec} and non-polar E_{vdW} interaction contributions by each sugar moieties is illustrated in Fig. 4 left panel. For both 1918 HA and 2009 HA, the largest contribution, be it electrostatic or non-polar, to the binding interaction comes from Sia 1 with over 50% of the total interaction energy for the whole ligand. This observation indicates that Sia 1 plays a key role in the binding process. The high electrostatic contribution from Sia 1 can be explained by its extensive hydrogen bonding and the high non-polar contribution by its relatively large volume, when compared to the other three sugar moieties (refer to Fig. 4 right panel). Considering the change in value from 1918 to 2009, the graph also shows that there is a larger change in contributions by Sia 1 and Gal 4 (around 4% for electrostatic and 9% for non-polar) to the overall interaction energy, relative to the changes in contributions by Gal 2 and Glc-NAc 3 (around 1% for electrostatic and 3% for non-polar). Comparing the two interaction energy components across the sugar

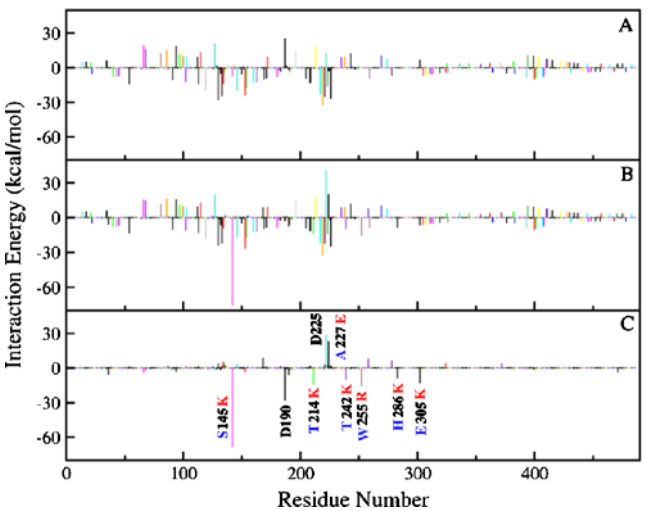

Fig. 5 Interaction spectrum ($E_{vdW+elec}$) of **a**) 1918 complex, **b**) 2009 complex, and **c**) the difference ($E_{2009} - E_{1918}$). Mutations are denoted as "1918 residue – residue number – 2009 residue"

moieties, the non-polar contribution seems to have larger percentage changes compared to the electrostatic contribution.

The results of hydrogen bond analysis are summarized in Fig. 4 right panel. Out of the four sugar moieties, only Sia 1 has all its hydrogen bonds preserved. This observation agrees with the calculated interaction energy components obtained. From Fig. 4 left panel, values for electrostatic contribution by Sia 1 in 1918 and 2009 HAs are relatively similar (67.29% and 63.45%, respectively), indicating minimal change in the electrostatic binding interaction.

The interaction spectrum between individual residues and the human receptor molecule is also illustrated in Fig. 5. This spectrum provides an easy means to extract molecular insight of protein-ligand binding by explicitly calculating the interaction energy ($E_{vdW+elec}$) between individual residues and ligand. The detailed quantitative information about specific residue interaction with the human receptor molecule should be extremely useful to our understanding of the molecular nature of 2009 H1 HA-human receptor binding. In Fig. 5, frame C shows the difference in interaction energy between the 1918 and 2009 complex ($E_{2009} - E_{1918}$) against the residue number. There are 9 residues that create significant change in the interaction energy, out of which 7 have undergone mutation in the 2009 complex. The data suggests that the mutations have contributed to the more favorable binding of hemagglutinin to the human receptor molecule. Comparing the data in Frame C with that in Fig. 4 right panel, the highly negative value for S145K can partly be explained by the newly-formed hydrogen bond between that residue to Sia 1 (with 25.37% occupancy) in the 2009 complex; the negative value for D190 by a newly-formed hydrogen bond to Gal 2, Glc-NAc 3, and Gal 4 each, overshadowing the decrease in percentage occupancy of the existing bond with Glc-NAc 3; the positive value for D225 by the loss of a hydrogen bond and a decrease in percentage occupancy in another bond to Gal 2. The other six residues which cannot be accounted for in Fig. 4 may have other forms of interaction, apart from hydrogen bond, to the human receptor molecule. The contribution from non-polar interaction may not be as much as that from electrostatic interaction in the case of these 9 residues because the majority of them, except A227 and W255 in 1918 complex, are polar residues.

Conclusions

This study attempted to provide the much needed information on the molecular dynamic behavior of human receptor molecule as well as its individual sugar moieties in the hemagglutinin of 1918 and 2009 H1N1 virus. Sialic acid seems to be the most important sugar moiety in the human receptor for the hemagglutinin to bind with, possibly because of its position as the outermost sugar moiety which allows more degree of freedom to fit into the binding site compared to the other three sugar moieties. Hence, in our search for analogs of human receptor molecule, perhaps it would be better to have minimum changes in sialic acid and modify the other three sugar moieties instead [23–25]. Moreover, from the interaction spectrum, we observe that six of the mutated residues in the 2009 glycan binding domain give more attractive interactions with the same human receptor molecule. Such detailed quantitative information on individual residue-human receptor interaction energy gives insight into molecular mechanism in hemagglutinin-human receptor binding and provides a useful and practical tool in rational design of hemagglutinin inhibitors. We hope that with the information acquired from this study, possible analogs of the human receptor can be proposed with greater confidence to develop more potent hemagglutinin inhibitors and eventually, a better drug for H1N1 influenza treatment.

Acknowledgments DWZ is supported in part by Nanyang Technological University start-up grant, and in part by Singapore AcRF Tier 1 Grant of M52110095. DWZ would like to acknowledge and thank NTU HPC support and resources.

References

1. Wiley DC, Skehel JJ (1987) The Structure and Function of the Hemagglutinin Membrane Glycoprotein of Influenza Virus. Ann Rev Biochem 56:365–394
2. Skehel JJ, Wiley DC (2003) Receptor binding and membrane fusion in virus entry: The Influenza Hemagglutinin. Ann Rev Biochem 69:531–569
3. Bucher D, Palese P (1975) The biologically active proteins of influenza virus: neuraminidase. Academic, New York
4. Palese P, Tobita K, Ueda M, Compans RW (1974) Characterization of temperature sensitive influenza virus mutants defective in neuraminidase. Virology 61:397–410
5. Neumann G, Noda T, Kawaoka Y (2009) Emergence and pandemic potential of swine-origin H1N1 influenza virus. Nature 459:931–939
6. World Health Organization (2010) Global Alert and Response (GAR) - Pandemic (H1N1) 2009. http://wwwwhoint/csr/disease/swineflu/en/ (accessed 13 July 2010)
7. US Food and Drug Administration (2010) Influenza (Flu) antiviral drugs and related information. http://wwwfdagov/Drugs/DrugSafety/InformationbyDrugClass/ucm100228htm#ApprovedDrugs (accessed 13 July)
8. Hancock K, Veguilla V, Lu X, Zhong W, Butler EN, Sun H, Liu F, Dong L, DeVos JR, Gargiullo PM, Brammer TL, Cox NJ, Tumpey TM, Katz JM (2009) Cross-reactive antibody responses to the 2009 pandemic H1N1 influenza virus. N Engl J Med 361:1945–1952
9. Itoh Y, Shinya K, Kiso M, Watanabe T, Sakoda Y, Hatta M, Muramoto Y, Tamura D, Sakai-Tagawa Y, Noda T, Sakabe S, Imai M, Hatta Y, Watanabe S, Li C, Yamada S, Fujii K, Murakami S, Imai H, Kakugawa S, Ito M, Takano R, Iwatsuki-Horimoto K, Shimojima M, Horimoto T, Goto H, Takahashi K, Makino A,

Ishigaki H, Nakayama M, Okamatsu M, Takahashi K, Warshauer D, Shult PA, Saito R, Suzuki H, Furuta Y, Yamashita M, Mitamura K, Nakano K, Nakamura M, Brockman-Schneider R, Mitamura H, Yamazaki M, Sugaya N, Suresh M, Ozawa M, Neumann G, Gern J, Kida H, Ogasawara K, Kawaoka Y (2009) In vitro and in vivo characterization of new swine-origin H1N1 influenza viruses. Nature 460:1021–1025

10. Xu R, Ekiert DC, Krause JC, Hai R, Crowe JE Jr, Wilson IA (2010) Structural basis of preexisting immunity to the 2009 H1N1 pandemic influenza virus. Science 328:357–360
11. Liu J, Stevens DJ, Haire LF, Walker PA, Coombs PJ, Russell RJ, Gamblin S, Skehel JJ (2009) Structures of receptor complexes formed by hemagglutinins from the asian influenza pandemic of 1957. Proc Nat Acad Sci 106:17175–17180
12. Maestro version 80 Schrödinger LLC New York NY 2007
13. Case DA, Darden TA, Cheatham Simmerling CL, Wang J, Duke RE, Luo R, Merz KM, Pearlman DA, Crowley M, Walker RC, Zhang W, Wang B, Hayik S, Roitberg A, Seabra G, Wong KF, Paesani F, Wu X, Brozell S, Tsui V, Gohlke H, Yang L, Tan C, Mongan J, Hornak V, Cui G, Beroza P, Mathews DH, Schafmeister C, Ross WS, Kollman PA (2006) Amber 9
14. Duan Y, Wu C, Chowdhury S, Lee MC, Xiong G, Zhang W, Yang R, Cieplak P, Luo R, Lee T, Caldwell J, Wang J, Kollman P (2003) A point-charge force field for molecular mechanics simulations of proteins based on condensed-phase quantum mechanical calculations. J Comput Chem 24:1999–2012
15. Kirschner KN, Yongye AB, Tschampel SM, González-Outeiriño J, Daniels CR, Foley BL, Woods RJ (2008) GLYCAM06: a generalizable biomolecular force field carbohydrates. J Comput Chem 29:622–655
16. Ryckaert JP, Ciccotti G, Berendsen HJ C (1977) Numerical integration of the cartesian equations of motion of a system with constraints: molecular dynamics of n-alkanes. J Comput Phys 23:327–341
17. Berendsen HJC, Postma JPM, van Gunsteren WF, DiNola A, Haak JR (1984) Molecular dynamics with coupling to an external bath. J Chem Phys 81:3684–3690
18. Humphrey W, Dalke A, Schulten K (1996) VMD: visual molecular dynamics. J Mol Graph 14:33–38
19. Cui Q, Sulea T, Schrag JD, Munger C, Hung MN, Naïm M, Cygler M, Purisima EO (2008) Molecular dynamics–solvated interaction energy studies of protein-protein interactions: the MP1–p14 scaffolding complex. J Mol Biol 379:787–802
20. Naïm M, Bhat S, Rankin KN, Dennis S, Chowdhury SF, Siddiqi I, Drabik P, Sulea T, Bayly CI, Jakalian A, Purisima EO (2007) Solvated interaction energy (SIE) for scoring protein−ligand binding affinities 1 exploring the parameter space. J Chem Inf Model 47:122–133
21. Åqvist J, Medina C, Samuelsson JE (1994) Protein Eng 7:385
22. ChemBioDraw Ultra 11 Cambridgesoftcom 100. Cambridge Park Drive, Cambridge MA, 02140 USA
23. Cheng XM, Liu XW (2007) Microwave-assisted one-pot synthesis of 3-acyl-5-hydroxybenzofurans. J Comb Chem 9:906–908
24. Yang RL, Pasunooti KK, Li FP, Liu XW, Liu CF (2009) Dual native chemical ligation at lysine. J Am Chem Soc 131:13592–13593
25. Gorityala BK, Cai ST, Lorpitthaya R, Ma JM, Pasunooti KK, Liu XW (2009) A convenient synthesis of pseudoglycosides by metal-free H3PO4 catalyst. Tetrahedron Lett 50:676–679